



# Pressuremeter Testing Along Interstate 10 in Tucson, Arizona

**Naresh C. Samtani**, President, NCS GeoResources, LLC, Tucson, USA; email: [naresh@ncsgeoresources.com](mailto:naresh@ncsgeoresources.com)

**ABSTRACT:** In arid to semi-arid regions alluvial soil deposits can range from collapse-susceptible, variably cemented to indurated. In these soils, reliable estimation of soil properties based on penetration resistance indicators such as N-values from Standard Penetration Tests (SPTs) is difficult. Varying content of gravels and cobbles provides additional complexity. In such conditions, sample recovery from SPTs is limited and refusal N-values occur. This paper presents a database of 74 pressuremeter tests along portions of Interstate 10 (I10) through Tucson, Arizona, where soil conditions noted above were encountered. The results are used to evaluate the subsurface stratigraphy. Estimated side and base resistance for drilled shafts are presented and compared with recommendations by the American Association of State Highway and Transportation Officials (AASHTO) and the Federal Highway Administration (FHWA). Comparisons of estimated side and base resistances from pressuremeter tests with those from a large-scale load test are presented. Evaluation of the collapse potential of soils using pressuremeter tests is also discussed and the results compared with collapse potential based on 1-D laboratory tests.

**KEYWORDS:** Pressuremeter, Cementation, Induration, Alluvial Soils, Interstate 10, Drilled Shaft, Side Resistance, Base Resistance, Collapse Potential

**SITE LOCATION:** [Geo-Database](#)

## INTRODUCTION

Interstate 10 (I10) stretches from Florida to California and is a major east-west commerce route in the US. The location of I10 through Arizona is shown on Figure 1a. Between Phoenix and Tucson, the I10 has a northwest-southeast direction. In Phoenix, the I10 is a part of a network of freeways. However, through Tucson, it is the only freeway. In south Tucson, I10 connects to Interstate 19 (I19) via a Traffic Interchange (TI), i.e., the I10-I19 TI. The I19 connects to the border port of Nogales and provides a key corridor for trade with Mexico. With the anticipated increase in population and traffic volumes, the Arizona Department of Transportation (ADOT) in the early 1990s initiated the process of reconstructing the I10-I19 TI and I10 through Tucson. The reconstruction of the I10-I19 TI was completed in 2003. Since then the I10 through Tucson has been undergoing reconstruction proceeding northward from I10-I19 TI towards Phoenix. Several new TIs have been constructed to date and several more are planned for reconstruction over the next decade.

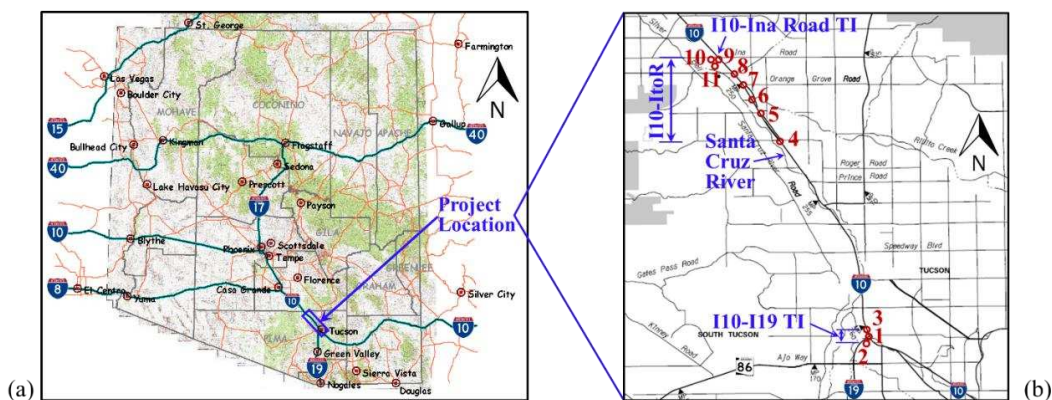


Figure 1. (a) Project location in Arizona, and (b) Location of pressuremeter tests (base map from PAG, 2019)

Submitted: 15 July 2019; Published: 11 May 2020

Reference: Samtani, N. C. (2020). Pressuremeter Testing Along Interstate 10 in Tucson, Arizona, International Journal of Geotechnical Engineering Case Histories, Vol.5, Issue 3, p. 152 - 169. doi: [10.4417/IJGCH-05-03-02](https://doi.org/10.4417/IJGCH-05-03-02)



The numbers on Figure 1b indicate the locations where pressuremeter tests were performed. The locations are numbered from south at the I10-I19 TI to the north at the I10-Ina Road TI. Because of the distinct clustering of the locations, Locations 1 to 3 are collectively referred to as the I10-I19 TI location while Locations 4 to 11 are collectively referred to as I10-ItoR location where “ItoR” denotes Ina Road to Ruthrauff Road. Table 1 provides a summary of the pressuremeter tests. The pressuremeter tests were performed to assist in characterizing the stiffness and volume change properties of the soils at the locations noted in the Column (Col) 3 of Table 1. A total of 88 pressuremeter tests were attempted from which 14 tests were found to be unusable primarily due to the test hole being too big or disturbed (e.g., due to sloughed soils). The distribution of the 74 usable tests at various locations is noted in Col 7. The number of the table in this paper where the pressuremeter data for each of the tests are included is identified in Col 8. In addition to presenting the results of the pressuremeter tests and interpreting the test results for site characterization, estimated values of side and base resistance for drilled shafts (bored concrete piles) as well as collapse potential of soils are also presented in this paper. The pressuremeter tests at I10-I19 TI location were performed in 1999-2000 while those at I10-ItoR location were performed in 2011-2012.

Table 1. Summary of Pressuremeter tests.

Location Number	Collective Location	Specific Location	Test Hole	Latitude	Longitude	Number of Tests	Data Table
Col 1	Col 2	Col 3	Col 4	Col 5	Col 6	Col 7	Col 8
1	I10-I19 TI	Center part of I10-I19 TI	PM-1	32°11'43.20"N	110°58'43.53"W	8	3
2		South part of I10-I19 TI	PM-2	32°11'22.12"N	110°58'54.05"W	5	4
3		North part of I10-I19 TI	PM-3	32°11'58.27"N	110°58'45.58"W	3	5
4	I10-ItoR	I10-Ruthrauff Road TI	PRM-RU	32°17'40.68"N	111°01'41.84"W	11	6
5		I10-Sunset Road TI	PRM-SU	32°18'31.68"N	111°02'31.93"W	10	7
6		I10 bridges over Rillito Creek	PRM-RI	32°18'54.85"N	111°02'44.90"W	6	8
7		I10-Orange Grove Road TI	PRM-OG	32°19'23.34"N	111°03'07.79"W	9	9
8		I10 bridges over CDO Wash	PRM-CD	32°19'43.77"N	111°03'22.33"W	6	10
9		I10-Ina Road TI	PRM-IN	32°20'13.77"N	111°04'02.79"W	11	11
10		I10-Ina Road TI	PRM-IN2	32°20'13.78"N	111°04'02.93"W	3	12
11		I10-Ina Road TI	PRM-IN3	32°20'13.72"N	111°04'02.81"W	2	13

## REGIONAL GEOLOGY AND SOIL UNITS

The Tucson region is semi-arid and the I10 through Tucson is in the northwestern part of the Tucson Basin which is a broad 2,600 km<sup>2</sup> area in the upper Santa Cruz River (SCR) drainage basin located in Pima County, Arizona. The Tucson basin is filled with alluvial deposits eroded from the surrounding mountain ranges. As shown in Figure 1b, the I10 in Tucson region roughly parallels the SCR. The SCR is about 0.8 km east of I10-I19 TI and about 1 km west of I10-Ina Road TI. Based on Parker (1995), the stretch of I10 shown in Figure 1b lies within the meander limits of the SCR. The near-surface soils include overbank deposits of silt, clay and fine sand, and channel deposits comprised of sand, gravel and cobbles transported from the surrounding mountains and alluvial terraces. The United States Geological Survey (USGS) identified these near-surface soils as Recent Alluvium (“Qal”) unit and noted that they are randomly layered within the soil profile as a result of thousands of years of the SCR channel meandering (Davidson, 1973; Anderson, 1987). Below the Qal unit lie older alluvial terrace deposits comprised of sand and gravel with varying amounts of clay, cobbles and boulders. USGS (Davidson, 1973; Anderson, 1987) indicates these older units are part of the Fort Lowell Formation (“Qf”) and Upper Tinaja bed (“Tsu”). Based on the information in Anderson (1987), deposition in Tucson Basin was punctuated by periods of erosion and/or nondeposition. These events led to formation of soils with varying cementation which in geotechnical literature (e.g., Nowatzki and Almasmoum, 1988) is attributed to salts left within the soil matrix during moisture migration phenomena such as evaporation of descending surface water or evaporation of ascending groundwater. These events also led to varying levels of induration and varying profiles of soil suction leading to a complex stress state and stress history.

## CONVENTIONAL GEOTECHNICAL INVESTIGATION PROGRAMS

Conventional geotechnical investigation programs were first implemented at each collective location. These programs consisted of field testing that included Standard Penetration Tests (SPTs) in test holes and laboratory testing that included evaluation of soils for engineering classification, index properties, collapse potential, electrochemical properties, shear strength, volume change, etc. The test holes were drilled using CME-75 truck-mounted drill rigs with 108 mm inside diameter (I.D.) and 206.4 mm outside diameter (O.D.) hollow-stem augers (HSA). At the I10-I19 TI location, SPTs were performed at 1.5 m vertical intervals in 173 test holes with depths ranging from 1.5 to 45 m. Supplementary investigations included



pressuremeter tests, sacrificial demonstration shafts to evaluate means and methods to excavate production shafts, and an Osterberg cell (O-cell) axial load test on a 2.44 m diameter and 41.1 m long drilled shaft that established a world record at that time in terms of applied equivalent top-down load of 150 MN (Samtani and Liu, 2005). For the I10-ItoR location, SPTs were performed at 1.5 m intervals in 347 test holes with depths ranging from 1.5 to 45 m. Supplementary investigations included pressuremeter tests. Thus, overall, the data from pressuremeter tests reported in this paper were interpreted with data from 520 test holes, laboratory tests, demonstration shafts, and a large-scale axial load test.

## GENERALIZED SUBSURFACE CONDITIONS

The reconstruction of the I10 is within the footprint of the original I10 corridor. Thus, embankment fills were found at all locations. Below the fills, it was difficult to identify distinct continuous strata of soils with specific Unified Soil Classification System (USCS) designations (e.g., SP, CL, etc.). This is to be expected because of the thousands of years of meandering of the SCR within the footprint of which the entire I10 corridor shown in Figure 1b occurs. Soil types ranged from fine-grained to coarse-grained as is typical for alluvial deposits. The meandering process led to random intermixing of these soils. Except for organic soils (OL, OH) and high plasticity silts (MH) that were not encountered, soils observed during field and laboratory investigations encompass the entire spectrum of soil designations in USCS as described in ASTM D 2487. Random lake-bed and gravel deposits dating to the Holocene and Pleistocene ages were also found.

From a geotechnical perspective, based on empirical correlations of SPT N-values with density and consistency, the subsurface conditions can be generalized into 3 layers as shown in Figure 2. Layer 1 includes the upper 8 to 10 m of the natural soils below the fills and contains generally loose to medium dense collapse-susceptible soils. At the I10-I19 TI, lenses of strongly cemented soils were encountered in this layer. These soils are part of the Qal unit. The lowest layer, Layer 3, includes dense to very dense soils with sub-angular to angular particles and is typically encountered at a depth below about 35 m. In Layer 3, refusal N-values (i.e., blows greater than 50 for sampler penetration less than 150 mm) were predominant giving the impression that it is the strongest of the three layers from a geotechnical strength perspective. The refusal N-values are not only due to the density but also presence of gravel and cobbles. At both collective locations, within Layer 3, localized pockets of fine-grained soils with SPT N-values in 20s to 30s were encountered. Layer 3 soils are part of the Tsu unit. Between the relatively well-defined Layer 1 and Layer 3, is the Layer 2 where a larger variation in soil characteristics was observed and location-specific sub-layers could be characterized. For example, at the I10-I19 TI location, Layer 2 included two 1 to 2 m thick sub-layers of stiff to very stiff clay above and below a generally medium dense to dense coarse-grained sub-layer. In contrast, at the I10-ItoR location medium dense to dense coarse-grained soils without the bounding clay sub-layers were found. In Layer 2 (in contrast to Layer 3), the coarse-grained soils have particles that are sub-rounded to rounded. Below the lower clay layer at I10-I19 TI, a strongly cemented sub-layer of gravelly soils that is “rock-like” in texture and resembles conglomerate was encountered. In addition to the calcium carbonate (CaCO<sub>3</sub>) cementation, calcite (CaO) crystals were encountered in this “rock-like” layer. Overall, Layer 2 and its sub-layers are part of the Qf unit and refusal N-values were often encountered in this layer.

Bedrock or regional groundwater was not encountered within the depth of exploration. Perched groundwater in 7 (out of 173) test holes was encountered above the upper clay layer at I10-I19 TI location and in none of the 347 test holes at the I10-I2R location. As per the criteria in ASTM D 2488 for describing moisture condition, other than in the perched groundwater zones, the soils within the depth of exploration were “dry” which means “absence of moisture, dusty, dry to touch.” Thus, from a geotechnical perspective, soils within the depth of exploration can be considered drained.

Layer	General Characteristics	
1	8-10 m	Loose to medium dense collapse-susceptible soils. Lenses of strongly cemented soils.
2	25-27 m	Intermixed alluvial soils that are variably cemented. Discontinuous sub-layers of stiff to very stiff clay towards the top and bottom of this layer that encompass generally medium dense to dense coarse-grained soils. Particles are generally rounded to sub-rounded. Cementation varies from weak to strong.
3	Below @ 35 m	Dense to very dense soils with subangular to angular particles. Predominately refusal N-values. Larger gravel and cobble content. Localized pockets of softer fine-grained soils.

Figure 2. Generalized subsurface stratigraphy.



## DESCRIPTION OF CEMENTED SOILS

The tested soils exhibited varying levels of cementation. In the field, the cementation of coarse-grained soils is described according to the criteria in ASTM D 2488 as follows: weak: crumbles or breaks with handling or little finger pressure; moderate: crumbles or breaks with considerable finger pressure; strong: will not crumble or break with finger pressure. Resistance to crumbling under finger pressure can result from induration and/or chemical reactions between the soil particles and salts. Because  $\text{CaCO}_3$ , a salt, is a common cementing agent in soils, its observed reaction with dilute (10% concentration) hydrochloric (HCl) acid is described in the field according to the criteria in ASTM D 2488 as follows: none: no visible reaction; weak: some reaction, with bubbles forming slowly; strong: violent reaction, with bubbles forming immediately. Soils with  $\text{CaCO}_3$  are often referred to as “caliche” or “marl.” A useful classification system for caliche is included in Table 2 and its terminology is used in this paper.

Table 2. Classification of Caliche (adapted from Nowatzki and Almasmoum, 1998).

Degree of Induration	Descriptive Hardness	Hardness Test		Unconfined Compressive Strength, $q_u$ , MPa	Ease of Sampling
		Break with hammer	Score with knife		
Very high	Extremely hard	Difficult	Difficult	21 to 55	Difficult
High	Very hard	Easy	Difficult	5 to 20	Difficult
Moderate	Hard	Easy	Easy	1 to 5	Moderately difficult
Slight	Moderately hard	Easy	Easy	<1	Easy
None	Soft to hard	Easy	Easy	<0.2 to 5.5	Easy to difficult

At the I10-I19 TI, two distinct zones with elevated  $\text{CaCO}_3$  content were noted, one within 0 to 11 m from the ground surface and the other between depths of about 20 to 30 m (Samtani and Liu, 2005). Based on observations of physical samples, the lower zone differs from the upper zone in that it contains a sub-layer which is “extremely hard” caliche, resembles conglomerate noted earlier, and is likely an ancient erosional surface on which the overlying alluvial soils were deposited. At other depths where soils were observed to be strongly cemented with strong reaction to HCl, lenses of “hard” to “very hard” caliche were found at I10-I19 TI. In these instances, rock core barrels were needed to drill test holes and shafts through these zones.

At other depths at I10-I19 TI locations as well as I10-ItoR locations the reaction of soils to HCl acid were observed to be “weak” to “none.” There were instances where the HCl reaction was “strong” but the cementation was “weak” which suggests that the soil particles are coated with  $\text{CaCO}_3$  but the voids are mostly clear, i.e., the particles are not significantly cemented to each other. Cases where the cementation was “weak,” HCl reaction was “none,” but the SPT N-value was relatively high (e.g., >30) could be indicative of the effect of induration, presence of cobbles or boulders, some other form of chemical cementation, and/or soil suction. Such instances were often encountered at all locations. The Notes column in Tables 3 through 13 provide letter codes for the observed levels of cementation and reaction to HCl acid at each pressuremeter test location. Because the ASTM designation of “weak” cementation includes the possibility of sample crumbling under handling, cases where no cementation was observed, the letter code “W” has been used for cementation.

## THE PRESSUREMETER AND TEST PROCEDURES

All pressuremeter tests were performed using the mono-cell Menard G-Am pressuremeter system manufactured by RocTest with the maximum pressure capacity of 9.6 MPa. The cylindrical probe has a diameter of 70 mm (N size) and contains an expandable rubber membrane (measuring cell) and a contiguous independently expandable guard cell. The length of the measuring cell is 380 mm, thus giving a length to diameter ratio of 5.4. The pressuremeter tests were performed in test holes that were drilled with HSA as noted earlier. SPTs were first performed in the test holes. The soil cuttings retrieved from the SPT spoon samples were logged according to the USCS to permit an evaluation of the types of geomaterials in which the pressuremeter tests were performed. Pressuremeter tests were conducted in test pockets (smaller diameter test holes) made at the bottom of the HSA string to an additional depth of about 1.2 to 1.5 m by using one of the following three methods.

1. A 1.5 m long, 76.2 mm diameter solid flight auger attached to a string of A-size drill rods.
2. Pushing 2 or 3 sequential 457.2 mm long, 63.5 mm I.D., 76.2 mm O.D. thick-walled ring samplers.
3. A 74.6 mm tricone rockbit and N-size drill rod, with air as a drilling fluid.



The choice of the method depended on the type of geomaterials encountered. The solid flight auger was better suited for gravelly soils. For softer or loose soils, the ring sampler approach was used but was found to generate more disturbed test pockets based on observation of slough and relatively high levels of hole wall disturbance that was also reflected in the test results. The tri-cone rockbit generally resulted in better test pockets regardless of the type of geomaterial. The diameter of the hole in which a pressuremeter test was conducted was approximately 76 mm, which is within the diameter tolerance (more than 1.03 times the probe diameter [72.1 mm] and less than 1.2 times the probe diameter [84.1]) as recommended by ASTM D 4719. The hole diameter of approximately 76 mm was estimated based on the observation that the probe engaged the sides of the test pocket with minimal expansion. Consistency of processes across all the tests was provided by use of the same driller (Geomechanics Southwest, Inc.), pressuremeter equipment noted above, tester (Dale Baures), and logging and testing procedures.

Immediately after the pressuremeter test pocket was prepared, the pressuremeter probe was lowered to the designated testing depth. The tests were performed in general accordance with the recommendations of ASTM D 4719. Specifically, a pressuremeter test was performed by expanding the probe in equal pressure increments and measuring the change in volume of the measuring cell with time for each increment. For a given pressure, volume readings were taken at 15, 30, and 60 seconds for the standard short-term test that models undrained (total stress) conditions. Because the soils at pressuremeter test depths were categorized as “dry” per ASTM D 2488, the test approaches drained conditions. An unload-reload cycle was typically included in the pressuremeter test. The raw pressure and volume change measurements obtained during the pressuremeter tests were corrected for inertia of the probe, expansion of the measurement system, and the hydraulic pressure of the column of fluid between the instrument and the measuring cell. Figure 3 shows plots for a typical pressuremeter test after appropriate corrections have been made to the raw data.

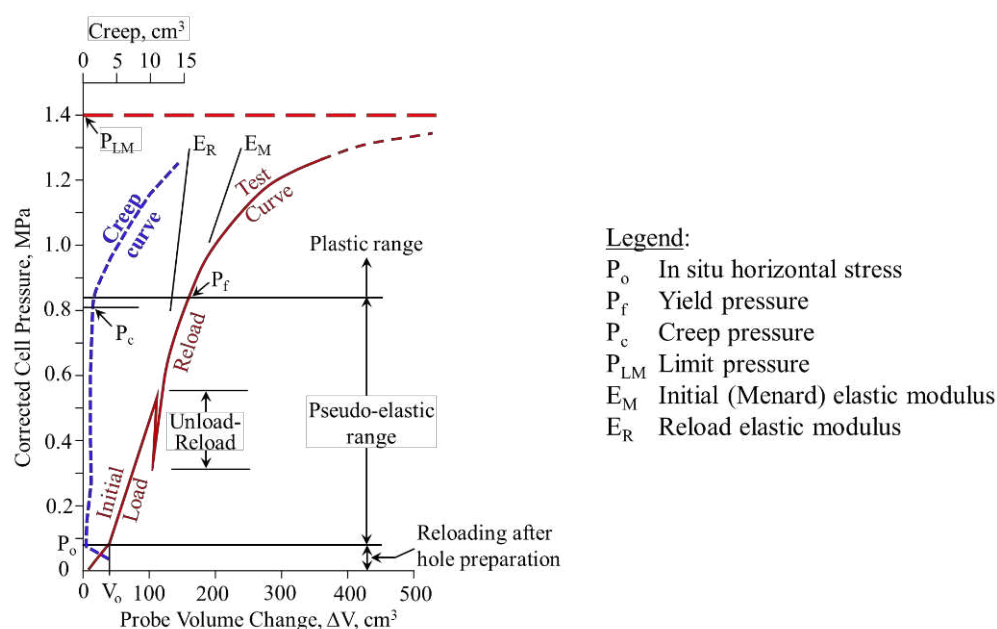


Figure 3: Schematic of Menard G-Am Pressuremeter test results (modified from Davidson, 1979).

Following are the various features of the typical pressuremeter test results shown in Figure 3:

1. In the initial reloading portion, the probe expands through the test hole and eventually meets the test hole walls and re-stresses the soil back to its in situ condition. The pressure in the probe,  $P_0$ , at this stage, commonly referred to as the seating pressure, is generally interpreted as the in situ horizontal stress.
2. In the linear pseudo-elastic range, the pressure increases from  $P_0$  to  $P_f$  at which the soil yields. The pressure  $P_f$ , termed the yield pressure, is useful in indicating the pressure beyond which significant long-term creep of the soil can occur.



3. Nonlinear deformation is exhibited in the plastic portion beyond  $P_f$ . The value corresponding to the asymptote to the plastic deformation curve is interpreted as the limit pressure,  $P_{LM}$ . The limit pressure,  $P_{LM}$ , is the pressure that doubles the initial test cavity volume (Briaud, 1992; Clarke and Gambin, 1998); this is also known as Menard's definition.
4. The slope of the linear portion of the initial portion of the test curve is used to calculate the initial shear modulus whereas the reload slope of an unload-reload test cycle is used to calculate the reload shear modulus. The corresponding elastic modulus values  $E_M$  (initial elastic modulus) and  $E_R$  (reload elastic modulus) are computed using the theoretical relation  $E=2G(1+\mu)$  where  $E$  is the elastic modulus,  $G$  is the shear modulus, and  $\mu$  is the Poisson's ratio. The  $E_M$  value is also referenced as the Menard modulus. The technique described by Gambin and Jézequel (1998) to estimate the initial modulus was used. Based on the type of soils encountered at the various locations,  $\mu=0.30$  was assumed.
5. The left dashed curve represents soil creep response where creep, as shown on the upper abscissa, is defined as the change in volume between 30 to 60 seconds at a given corrected cell pressure (i.e.,  $V_{60}-V_{30}$ , where  $V$  denotes volume and the subscript denotes time in seconds). The soil starts to yield when the value of creep begins to increase significantly at creep pressure,  $P_c$ , as shown in Figure 3. Typically,  $P_c$  was found to be close to  $P_f$  and therefore  $P_c=P_f$  was assumed because  $P_f$  was easier to evaluate from the pressure-volume change curve as it is better defined than the creep curve.

### Dry and Wet Pressuremeter Tests to Evaluate Collapse Potential

The tests performed using the processes described above are referred herein as “dry” tests which is intended to signify that the tests were performed without addition of any water before or during the tests. To evaluate the collapse potential of near surface soils, three “wet” pressuremeter tests were performed at depths of 2.3 m, 4.1 m, and 5.3 m at Location 9 (Ina Road, Test hole PRM-IN). These tests were paired with the “dry” pressuremeter tests performed at depths of 2.3 m, 3.8 m, and 5.3 m at Location 10 (Ina Road, Test hole PRM-IN2). The test holes at I10-Ina Road TI were spaced about 3 m apart to prevent the influence of drilling and testing in one test hole on the other. Because the surface elevations of Test holes PRM-IN and PRM-IN2 is the same (i.e., 669.6 m as noted in captions of Tables 11 and 12), comparison of the results of a pair of “wet” and “dry” tests at about the same depth in each of the two test holes permits an evaluation of the degree of severity of soil collapse under stress and moisture ingress. Hence, the pairs of “dry” and “wet” tests are referred to as the “dry and wet” tests. The difference between the “wet” and “dry” tests was the addition of water at the seating pressure during the “wet” tests in a manner similar to Procedure 2 noted in Smith and Rollins (1997). Specifically, the following steps were implemented during the “wet” tests: (1) Lower the probe in the test pocket, (2) expand the probe to the seating pressure,  $P_o$ , that is estimated from nearby dry tests conducted at about the same depths before the wet tests, (3) rapidly introduce 30 liters of water into the test hole through the HSA string, (4) measure change in volume of the probe and take readings at 0.25, 0.5, 0.75, 1, 1.5, 2, 2.5, 3, 3.5, 4, 4.5, 5 minutes and every minute afterwards until the probe volume is stabilized (i.e., volume change is negligible) in at least three consecutive time increments, (5) reduce the pressure in the probe to  $0.5P_o$  to permit water to migrate down the side of the test hole and wait about 30 secs for migration of the water to cease, (6) re-engage  $P_o$  in two steps, i.e.,  $0.75P_o$  and  $P_o$ , (7) take volume change readings at 0.5, 1, 2, 3, 4, 5, 10, 15, 20, 25 and 30 minutes, (8) increase probe pressure in 0.025 MPa ( $\approx 1/4$  bar) increments and perform the pressuremeter test to the limit pressure. Further discussion of the “dry and wet” test results is provided later.

### PRESSUREMETER TEST RESULTS

Tables 3 through 13 present a summary of the various parameters noted in Figure 3 based on pressuremeter tests performed at the locations identified in Table 1. The surface elevation of the test hole at each location is noted in the caption of each table. Information on the N-values and USCS soil designation is included in the second column of each table. A N-value of R denotes a refusal blowcount. The Notes column in each table provides letter and numeric codes which are explained in Table 14. Description of cementation and reaction to HCl acid, in accordance with ASTM D 2488, is provided via the first two letter codes, respectively, in the Notes column; e.g., W,S for the sample at depth of 2.4 m in Table 6 means the soils at that depth had “weak” cementation and “strong” reaction to HCl acid. The numeric codes range from 1 to 7 and provide additional information about the pressuremeter tests as identified in Table 14. Empty cells in the column for  $E_R$  indicate that unload-reload cycle was not possible for estimation of  $E_R$  because the test had to be terminated due to a numeric code condition identified in the “Notes” column. The other quantities,  $\sigma'_v$ ,  $K_o$ , LOCR,  $P_{NLM}$  and  $S_{NVC}$  are as follows:



- $\sigma'_v$  is the effective vertical overburden stress that was calculated based on the unit weights measured from laboratory tests during the conventional geotechnical investigation programs.
- $K_o$  is the coefficient of earth pressure at rest and is computed from  $K_o = P_o / \sigma'_v$ . It is an indicator of the state of in situ stress and stress history. During the test program, the tester estimated  $P_o$  while expanding the probe at the start of the test and observing the probe volume change as to when the rate of volume change decreases. After the test, during interpretation of the test results, the value of  $P_o$  was determined as the pressure corresponding to the initiation of linear elastic response in the initial load portion shown in Figure 3 as recommended by Davidson (1979).
- LOCR gives an indication of the overconsolidation ratio (OCR) in the lateral direction and is computed from  $LOCR = P_f / P_o$ . Traditionally, the OCR is computed from  $OCR = \sigma_p / \sigma'_v$  where  $\sigma_p$  is the preconsolidation stress in the vertical direction due to variety of past mechanisms (Brumund, et al. 1976). LOCR, as used herein, is used to evaluate potential influence of cementation and induration in the lateral direction. Like  $K_o$ , LOCR is also an indicator of stress history. The relationship between  $K_o$  and LOCR for a given test is  $LOCR = P_f / (K_o \sigma'_v)$ .
- $P_{NLM}$  is the net limit pressure obtained by subtracting  $P_o$  from  $P_{LM}$ . The value of  $P_{NLM}$  is less sensitive to the disturbance of the test hole wall which may occur during drilling (Baguelin et al., 1978; Briaud 1992) and is a measure of the soil strength that is used to develop design parameters for foundation design.
- $S_{NVC}$  is the no volume change shear strength that can be computed from the plastic failure portion of the pressuremeter curve. The  $S_{NVC}$  values were computed using the Gibson and Anderson (1961) procedure and provide an alternate indicator measure of the soil strength.

Profiles of  $K_o$ , LOCR,  $P_f$ ,  $P_{NLM}$  and  $S_{NVC}$  with respect to depth provide valuable information on relative changes within the subsurface that is useful to assess soil layering. Such profiles are presented and discussed in the next sections.

Table 3. Summary of Pressuremeter Tests – I10-I19 TI, Test Hole PM-1, Surface Elevation: 731.5 m.

Depth m	N-value (USCS) Blows/0.305 m (-)	$P_o$ MPa	$P_f$ MPa	$P_{LM}$ MPa	$E_M$ MPa	$E_R$ MPa	$\sigma'_v$ MPa	$K_o$ -	LOCR -	$P_{NLM}$ MPa	$S_{NVC}$ MPa	Notes -
4.0	42 (SW)	0.16	0.72	1.15	20.1	86.2	0.07	2.21	4.41	0.99	0.16	S,S
10.1	10 (CL)	0.23	0.64	1.34	10.1	81.4	0.19	1.20	2.79	1.11	0.18	M,S
15.8	R (GP-GC)	0.40	2.39	6.70	31.6,41.2	80.4	0.30	1.35	5.95	6.30	1.61	M,W,3
20.7	R (SC)	0.68	2.78	5.55	44.1	79.5	0.38	1.78	4.08	4.87	1.15	S,S
25.0	46 (CL)	0.74	2.59	5.55	42.1	59.4	0.47	1.57	3.51	4.82	1.24	S,S
32.3	R (SC)	0.79	6.22	12.45	64.2,186.7		0.61	1.30	7.83	11.65	2.49	S,S,3
37.5	134 (SC)	1.05	3.45	6.42	114.9	258.6	0.71	1.49	3.27	5.36	0.96	W,W
41.1	88 (SC)	1.08	2.97	6.80	155.1	325.6	0.79	1.38	2.74	5.72	0.98	W,W

Table 4. Summary of Pressuremeter Tests – I10-I19 TI, Test Hole PM-2, Surface Elevation: 729.2 m.

Depth m	N-value (USCS) Blows/0.305 m (-)	$P_o$ MPa	$P_f$ MPa	$P_{LM}$ MPa	$E_M$ MPa	$E_R$ MPa	$\sigma'_v$ MPa	$K_o$ -	LOCR -	$P_{NLM}$ MPa	$S_{NVC}$ MPa	Notes -
3.0	68 (SM)	0.12	1.44	3.45	35.4	134.1	0.06	2.17	11.54	3.32	0.62	S,S
11.1	78 (SW)	0.27	0.82	1.63	19.2	45.0	0.21	1.27	3.07	1.36	0.26	M,S
15.8	R (CL)	0.44	1.00	2.01	14.4	79.5	0.30	1.48	2.26	1.57	0.28	M,W
19.2	R (GP)	0.53	8.62	17.24	435.7	354.3	0.35	1.49	16.36	16.71	3.65	S,S
22.3	R (GP-GC)	0.56	3.83	7.95	72.8	44.1	0.41	1.37	70.80	7.38	2.60	S,S

Table 5. Summary of Pressuremeter Tests – I10-I19 TI, Test Hole PM-3, Surface Elevation: 727.6 m.

Depth m	N-value (USCS) Blows/0.305 m (-)	$P_o$ MPa	$P_f$ MPa	$P_{LM}$ MPa	$E_M$ MPa	$E_R$ MPa	$\sigma'_v$ MPa	$K_o$ -	LOCR -	$P_{NLM}$ MPa	$S_{NVC}$ MPa	Notes -
4.9	R (CL)	0.24	6.70	16.28	353.4	287.3	0.09	2.78	28.00	16.04	3.67	S,S
14.0	91 (SC)	0.56	2.11	65	54.1	109.2	0.26	2.15	3.79	5.67	1.27	M,W
20.4	37 (SC)	0.68	1.82	64	60.3	124.5	0.38	1.78	2.68	5.45	1.16	M,W



Table 6. Summary of Pressuremeter Tests – Ruthrauff Road, Test Hole PRM-RU, Surface Elevation: 685.0 m.

Depth m	N-value (USCS) Blows/0.305 m (-)	P <sub>o</sub> MPa	P <sub>f</sub> MPa	P <sub>LM</sub> MPa	E <sub>M</sub> MPa	E <sub>R</sub> MPa	σ' <sub>v</sub> MPa	K <sub>o</sub> -	LOCR -	P <sub>NLM</sub> MPa	S <sub>NVC</sub> MPa	Notes -
2.4	6 (SC)	0.03	0.27	0.48	6.4	24.1	0.05	0.57	10.37	0.45	0.08	W,S
3.8	15 (SM)	0.07	0.43	0.96	38.1	64.5	0.07	1.04	5.84	0.88	0.14	W,S
5.3	14 (SP)	0.08	0.59	1.15	12.4	63.7	0.10	0.77	7.75	1.07	0.18	W,N
6.9	13 (SP-SM)	0.06	0.60	1.20	13.9	114.9	0.12	0.49	9.69	1.13	0.17	W,N
11.0	R (GM)	0.11	0.74	1.48	6.8	70.8	0.20	0.52	7.00	1.38	0.24	W,N
17.5	R (SC)	0.37	1.92	3.83	136.4,89.3		0.33	1.10	5.13	3.46	0.56	W,N,1,3
19.5	40 (SC)	0.34	1.84	3.83	86.4	95.6	0.36	0.93	5.49	3.50	0.71	W,N
22.3	47 (SM)	0.34	3.86	7.76	114.9	151.3	0.41	0.80	11.51	7.42	1.62	W,N,1
28.3	57 (SC)	0.54	4.79	9.58	239.4		0.53	1.01	8.93	9.04	1.57	W,N,1
34.4	59 (SC)	0.46	2.87	5.75	67.8		0.65	0.71	6.25	5.29	1.07	W,N,1
39.0	70 (SC)	0.51	1.28	3.35	47.3	90.6	0.74	0.69	2.53	2.84	0.56	W,N,1

Table 7. Summary of Pressuremeter Tests – Sunset Road, Test Hole PRM-SU, Surface Elevation: 679.7 m.

Depth m	N-value (USCS) Blows/0.305 m (-)	P <sub>o</sub> MPa	P <sub>f</sub> MPa	P <sub>LM</sub> MPa	E <sub>M</sub> MPa	E <sub>R</sub> MPa	σ' <sub>v</sub> MPa	K <sub>o</sub> -	LOCR -	P <sub>NLM</sub> MPa	S <sub>NVC</sub> MPa	Notes -
2.1	10 (ML)	0.04	0.36	0.72	11.7	35.1	0.04	1.10	8.29	0.68	0.12	W,S
4.0	36 (ML)	0.07	0.58	1.20	35.3	55.9	0.07	0.92	8.70	1.13	0.20	W,S
9.6	13 (SW-SM)	0.05	0.49	1.01	6.9	42.3	0.18	0.29	9.25	0.95	0.16	W,N
14.2	R (GM)	0.16	0.38	0.77	5.8		0.26	0.61	2.38	0.61	0.11	W,N,1
16.5	R (SM)	0.26	2.60	5.27	118.7	239.4	0.31	0.86	9.85	5.00	0.89	W,N,1
20.4	R (SC-SM)	0.54	2.30	4.60	71.1		0.38	1.41	4.29	4.06	0.77	W,N,1
22.4	28 (SC)	0.52	2.14	4.31	143.6	252.2	0.42	1.25	4.12	3.79	0.62	W,N
26.5	65 (SC-SM)	0.23	0.75	1.63	45.2	77.4	0.49	0.46	3.29	1.40	0.24	W,N,2
31.4	R (SM)	0.86	1.43	2.87	354.3		0.59	1.45	1.66	2.02	0.25	W,N,1
35.5	R (SM)	1.02	1.78	3.64	73.7		0.67	1.53	1.74	2.61	0.45	W,N,2

Table 8. Summary of Pressuremeter Tests – Rillito Creek, Test Hole PRM-RI, Surface Elevation: 672.8 m.

Depth m	N-value (USCS) Blows/0.305 m (-)	P <sub>o</sub> MPa	P <sub>f</sub> MPa	P <sub>LM</sub> MPa	E <sub>M</sub> MPa	E <sub>R</sub> MPa	σ' <sub>v</sub> MPa	K <sub>o</sub> -	LOCR -	P <sub>NLM</sub> MPa	S <sub>NVC</sub> MPa	Notes -
13.1	R (SC-SM)	0.48	4.50	9.10	373.5	746.9	0.24	1.99	9.31	8.61	1.36	W,N,1,4
14.3	R (SC-SM)	0.20	2.39	4.79	114.9	229.8	0.27	0.76	11.90	4.59	0.80	W,N,1,4,5,6
17.2	R (SC-SM)	0.38	2.60	5.27	72.0	143.6	0.32	1.18	6.86	4.89	0.97	W,N,1,4
22.1	R (SW-SM)	0.38	3.27	6.51	51.0	102.5	0.41	0.93	8.59	6.13	1.42	W,N,4
28.2	83 (SW-SC)	0.71	5.52	11.49	526.7	1053.4	0.53	1.34	7.78	10.78	1.66	W,N,1,4
34.7	R (SC)	0.41	1.76	3.54	28.3,26.1	56.3	0.66	0.63	4.28	3.13	0.71	W,N,1,3

Table 9. Summary of Pressuremeter Tests – Orange Grove Road, Test Hole PRM-OG, Surface Elevation: 673.6 m.

Depth m	N-value (USCS) Blows/0.305 m (-)	P <sub>o</sub> MPa	P <sub>f</sub> MPa	P <sub>LM</sub> MPa	E <sub>M</sub> MPa	E <sub>R</sub> MPa	σ' <sub>v</sub> MPa	K <sub>o</sub> -	LOCR -	P <sub>NLM</sub> MPa	S <sub>NVC</sub> MPa	Notes -
2.4	16 (SM)	0.08	0.34	0.67	9.0	16.3	0.05	1.80	4.25	0.59	0.12	W,S
4.1	6 (SW-SM)	0.15	0.23	0.46	7.6	13.4	0.08	2.00	1.48	0.31	0.06	W,W
8.1	14 (SW-SM)	0.05	1.11	2.30	39.7	84.5	0.15	0.30	24.68	2.25	0.42	W,W
9.7	26 (SW-SM)	0.19	1.14	2.30	24.9	124.5	0.18	1.07	5.95	2.11	0.35	W,W
19.3	R (SM)	0.34	2.35	4.79	124.5	239.4	0.36	0.97	6.81	4.44	0.77	W,W
20.7	R (GW-GM)	0.28	3.55	7.18	249.0	325.6	0.38	0.74	12.58	6.90	1.23	W,N,1
23.5	R (SC)	0.25	2.08	4.21	229.8	258.6	0.43	0.58	8.19	3.96	0.66	W,N,1
28.7	R (SC-SM)	0.43	3.39	6.70	172.4		0.54	0.80	7.96	6.28	1.08	W,N,1
35.5	R (SC)	0.57	2.30	4.60	127.4	85.2	0.67	0.86	4.00	4.02	0.68	W,N



Table 10. Summary of Pressuremeter Tests – CDO Wash, Test Hole PRM-CD, Surface Elevation: 671.5 m.

Depth m	N-value (USCS) Blows/0.305 m (-)	P <sub>o</sub> MPa	P <sub>f</sub> MPa	P <sub>LM</sub> MPa	E <sub>M</sub> MPa	E <sub>R</sub> MPa	σ' <sub>v</sub> MPa	K <sub>o</sub> -	LOCR -	P <sub>NLM</sub> MPa	S <sub>NVC</sub> MPa	Notes -
13.0	43 (SW-SM)	0.17	0.55	1.15	12.3	23.9	0.24	0.70	3.30	0.98	0.20	W,N,1,4
16.0	R (GW-GM)	0.23	0.79	1.63	40.3	58.5	0.30	0.76	3.53	1.40	0.26	W,N
19.2	49 (SC)	0.36	4.16	8.43	74.0,196.3	507.5	0.36	1.00	11.65	8.07	1.34	W,N
23.8	R (SC)	0.44	2.20	4.40	159.9	167.6	0.44	1.00	5.00	3.96	0.72	W,N
28.5	R (SC)	0.62	0.99	1.96	14.8	30.6	0.53	1.16	1.59	1.34	0.29	W,N
42.4	25 (SC)	0.99	1.43	2.87	17.9	39.6	0.78	1.27	1.45	1.89	0.40	W,N,1

Table 11. Summary of Pressuremeter Tests – Ina Road, Test Hole PRM-IN, Surface Elevation: 669.6 m.

Depth m	N-value (USCS) Blows/0.305 m (-)	P <sub>o</sub> MPa	P <sub>f</sub> MPa	P <sub>LM</sub> MPa	E <sub>M</sub> MPa	E <sub>R</sub> MPa	σ' <sub>v</sub> MPa	K <sub>o</sub> -	LOCR -	P <sub>NLM</sub> MPa	S <sub>NVC</sub> MPa	Notes -
2.3	15 (CH)	0.02	0.21	0.45	13.8	31.8	0.04	0.38	13.18	0.43	0.07	M,S,7
4.1	7 (CL-ML)	0.06	0.21	0.42	6.3,17.4	23.5,22.7	0.08	0.75	3.62	0.36	0.06	W,W,7,3
5.3	9 (ML)	0.05	0.36	0.72	12.6,14.5	27.7	0.10	0.48	7.69	0.67	0.12	W,S,7,3
7.0	7 (CL)	0.05	0.55	1.10	37.6	76.2	0.13	0.41	10.53	1.05	0.17	W,S
10.1	17 (CL)	0.10	0.55	1.05	15.4	65.1	0.19	0.55	5.28	0.95	0.16	W,S,4
12.6	17 (GP)	0.11	0.57	1.15	14.1,7.3		0.23	0.49	5.00	1.03	0.17	W,N,1,3
18.8	71 (SC-SM)	0.31	2.20	4.60	114.0	239.4	0.35	0.88	7.19	4.29	0.74	W,N,1,4
20.4	27 (SC)	0.37	3.35	6.70	60.0		0.38	0.99	8.97	6.33	1.40	W,N,1
23.8	R (GC)	0.42	2.49	5.17	114.9		0.44	0.95	5.91	4.75	0.84	W,N,2
26.5	R (SM)	0.45	2.46	5.27	268.1	536.3	0.50	0.91	5.47	4.82	0.73	W,N
29.3	R (SC)	0.42	2.55	5.27	316.0		0.55	0.77	6.05	4.85	0.71	W,N,1

Table 12. Summary of Pressuremeter Tests – Ina Road, Test Hole PRM-IN2, Surface Elevation: 669.6 m.

Depth m	N-value (USCS) Blows/0.305 m (-)	P <sub>o</sub> MPa	P <sub>f</sub> MPa	P <sub>LM</sub> MPa	E <sub>M</sub> MPa	E <sub>R</sub> MPa	σ' <sub>v</sub> MPa	K <sub>o</sub> -	LOCR -	P <sub>NLM</sub> MPa	S <sub>NVC</sub> MPa	Notes -
2.3	7 (CL)	0.02	0.36	0.74	24.1	37.7	0.04	0.38	22.41	0.72	0.13	M,W
3.8	12 (CL)	0.06	0.38	0.72	21.1	61.9	0.07	0.81	6.67	0.66	0.10	M,S
5.3	5 (SM)	0.05	0.23	0.62	11.0	43.9	0.10	0.53	4.48	0.57	0.09	W,W

Table 13. Summary of Pressuremeter Tests – Ina Road, Test Hole PRM-IN3, Surface Elevation: 669.9 m.

Depth m	N-value (USCS) Blows/0.305 m (-)	P <sub>o</sub> MPa	P <sub>f</sub> MPa	P <sub>LM</sub> MPa	E <sub>M</sub> MPa	E <sub>R</sub> MPa	σ' <sub>v</sub> MPa	K <sub>o</sub> -	LOCR -	P <sub>NLM</sub> MPa	S <sub>NVC</sub> MPa	Notes -
37.5	R (GW-GC)	0.45	1.10	2.20	239.4	15.3	0.71	0.63	2.46	1.76	0.51	W,N
38.7	R (GW-GC)	0.36	1.06	2.15	4.8	17.0	0.73	0.50	2.92	1.79	0.51	W,N

Table 14. Codes for Notes Column in Tables 3 through 13.

Cementation (ASTM D 2488)		Reaction to HCl (ASTM D 2488)		Pressuremeter	
Code	Meaning	Code	Meaning	Code	Meaning
W	Weak	N	None	1	Outer membrane burst
M	Moderate	W	Weak	2	Inner membrane burst
S	Strong	S	Strong	3	2-layers within probe length
				4	Estimated value of E <sub>R</sub>
				5	Estimated value of P <sub>f</sub>
				6	Estimated value of P <sub>LM</sub>
				7	Wet test



## IN SITU STRESS STATE AND STRESS HISTORY

The in situ stress state and stress history was evaluated by studying the profiles of  $K_o$  and LOCR with depth. Figure 4 shows the profiles of  $K_o$  with depth at I10-I19 TI (Figure 4a) and I10-ItoR (Figure 4b). Figure 5 shows the profiles of LOCR with depth at I10-I19 TI (Figure 5a) and I10-ItoR (Figure 5b). In each figure, the charts for I10-I19 TI and I10-ItoR are drawn to the same scale to allow a direct comparison of trends.

The  $K_o$  value for normally consolidated soils can be computed based on effective friction angle,  $\phi'_f$ , using  $K_o = 1 - \sin\phi'_f$  (Jaky, 1944). The values of  $\phi'_f$ , for normally consolidated soils with USCS designations noted in Tables 3 through 13 typically range from 30 to 40 degrees. Therefore, the range of  $K_o$  values for normally consolidated soils would be approximately 0.35 to 0.50. Using this range of  $K_o$  as a reference, the following observations are made with respect to Figure 4.

- Based on the data in Figure 4a that are applicable to the I10-I19 TI it is noted that  $K_o > 1$  with the range being between approximately 1.2 to 2.8. Because at many of the locations at I10-I19 TI the cementation and reaction to HCl acid is strong, these large values of  $K_o$  reflect the combined effect of cementation and induration.
- Based on the data in Figure 4b that are applicable to the I10-ItoR,  $K_o$  ranges from approximately 0.3 to 2.0 with most of the values being between approximately 0.5 and 1.5. Because at many of the locations at I10-ItoR the reaction to HCl acid is weak to none, values of  $K_o$  larger than the range of 0.35 to 0.50 could be due to induration.
- For the I10-ItoR locations, a trend towards smaller  $K_o$  values below 35 m depth is observed.

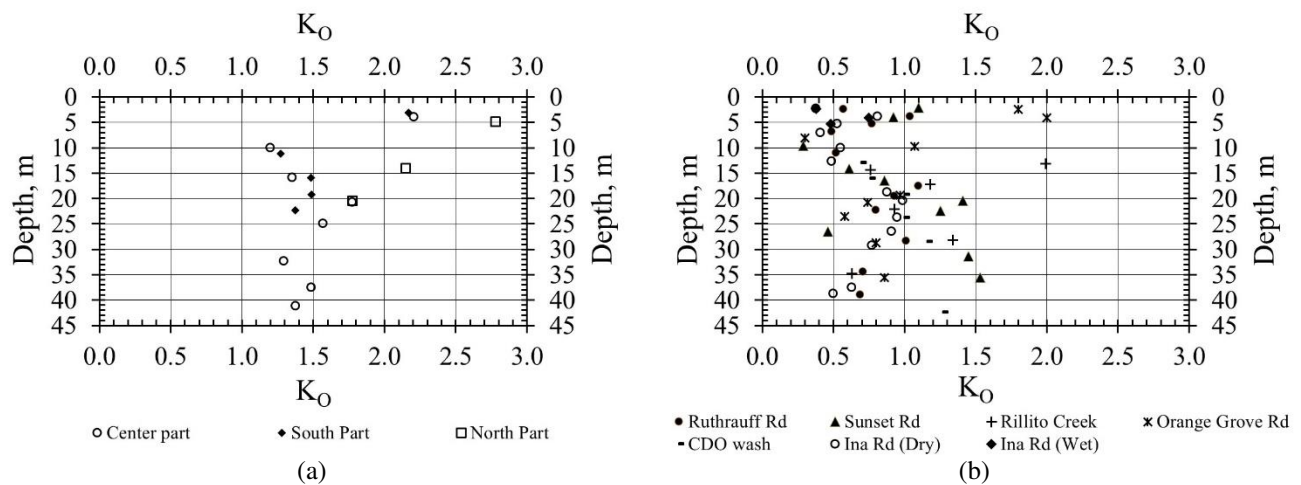


Figure 4.  $K_o$  profiles at (a) I10-I19 TI locations, (b) I10-ItoR locations.

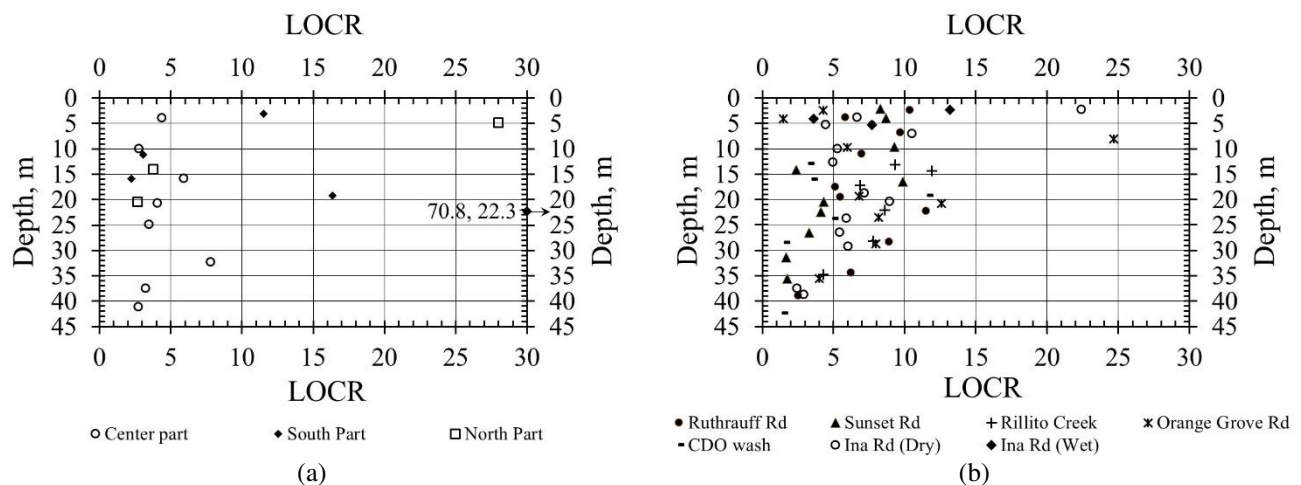


Figure 5. LOCR profiles at (a) I10-I19 TI locations, (b) I10-ItoR locations.



For normally consolidated soils, the value of LOCR is 1. The following observations are made with respect to Figure 5.

- Based on the data in Figure 5a that are applicable to the I10-I19 TI, LOCR ranges from approximately 2 to 70.8. Within this range, 4 of the 16 LOCR values are greater than 8. The  $K_o$  values corresponding to these points are also close to the higher end of their observed range noted earlier. These points correspond to locations where cementation and reaction to HCl is strong and physical observation of the samples at these locations indicated presence of hard to very hard caliche as discussed earlier. Overall, the values of  $LOCR > 1$  reflect the combined effect of cementation and induration.
- Based on the data in Figure 5b that are applicable to the I10-ItoR, LOCR ranges from approximately 1.5 to 25 with most of the values being between approximately 1.5 and 12. Because at many of the locations at I10-ItoR the reaction to HCl acid is weak to none, values of  $LOCR > 1$  could be due to induration.
- For the I10-ItoR locations, a trend towards smaller LOCR values below 35 m depth is observed.

The above observations that indicate magnitudes of  $K_o$  and LOCR are larger than those associated with normally consolidated soils are consistent with the depositional history of the alluvial soils in the Tucson Basin. Both  $K_o$  and LOCR are good indicators of the in situ stress state and stress history. Thus, the values of  $K_o$  and LOCR may be used in conjunction with the information on cementation and reaction to HCl included in the Notes column of Tables 3 to 13 to judge the effect of induration and cementation qualitatively. Such an evaluation can explain large values of side resistance that may be found in axial load tests (as noted later).

For a given test,  $LOCR = P_f / (K_o \sigma'_v)$ . Therefore, one may surmise a good correlation between  $K_o$  and LOCR. However as shown in Figure 6, the value of  $P_f$  varies considerably due to the randomness of cementation and induration at the test locations; this scatter is particularly noticeable between 10 and 35 m. Because  $K_o$  and LOCR are related through  $P_f$ , considerable scatter is also observed in plots of  $K_o$  versus LOCR included in Figure 7. These observations confirm the random alluvial soil depositional processes noted earlier in the discussion of regional geology and soil units.

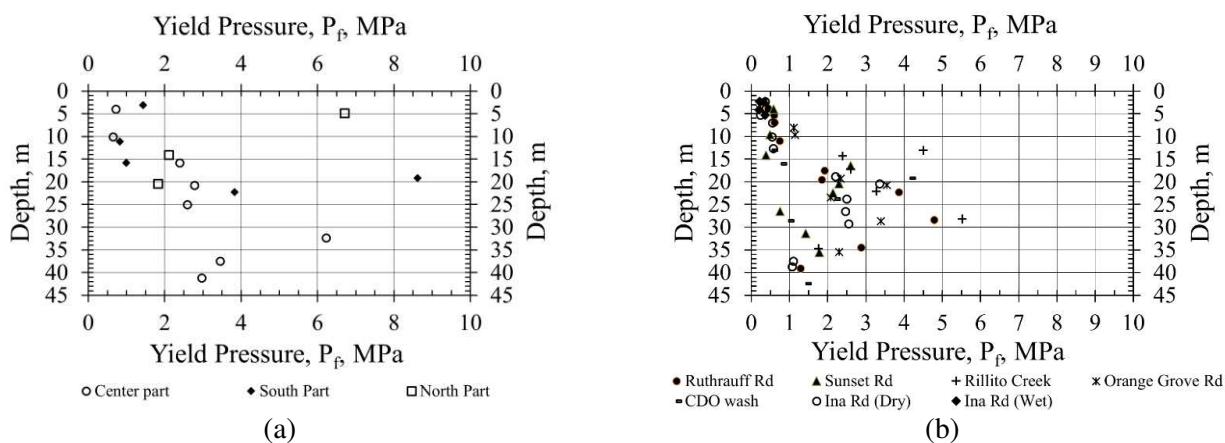


Figure 6.  $P_f$  profiles at (a) I10-I19 TI locations, (b) I10-ItoR locations.

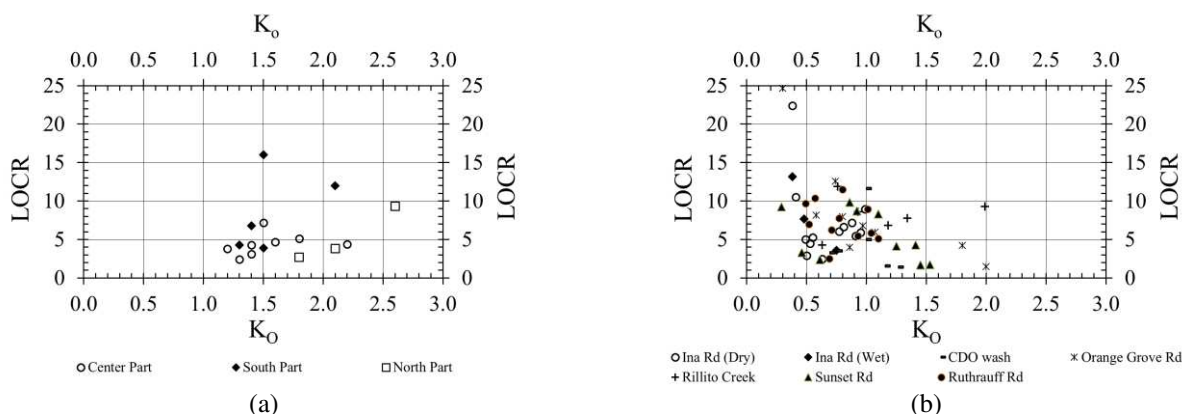


Figure 7.  $K_o$  vs LOCR at (a) I10-I19 TI locations, (b) I10-ItoR locations.



## PROFILES OF $P_{NLM}$ and $S_{NVC}$

Figures 8 and 9 show profiles of  $P_{NLM}$  and  $S_{NVC}$  with depth at the I10-I19 TI (Figures 8a and 9a) and I10-ItoR (Figures 8b and 9b) locations. In each figure, the charts for I10-I19 TI and I10-ItoR are drawn to the same scale to allow a direct comparison of trends. Both  $P_{NLM}$  and  $S_{NVC}$ , like  $P_f$ , are indicators of soil strength and their profiles with depth are useful to assess the soil layering from a geotechnical strength limit state perspective. The data trends in Figures 8 and 9 are like those for  $P_f$  in Figure 6 and suggest the following:

- Between depths of 10 m and 35 m, the values of  $P_{NLM}$  and  $S_{NVC}$  are larger than those above and below these depths.
- Except for some points at the I10-I19 TI location that corresponded to depths where strong cementation was encountered, the values of  $P_{NLM}$  and  $S_{NVC}$  in the upper 10 m are much smaller than those between depths of 10 m and 35 m.
- Below the depth of 35 m, the values of  $P_{NLM}$  and  $S_{NVC}$  are smaller in comparison to those between 10 m and 35 m.

Based on the above observations the following 3-layer system was surmised. Layer 1 from 0 to 10 m, Layer 2 from 10 to 35 m and Layer 3 below 35 m. These layers generally correspond to the Qal, Qf, and Tsu units noted earlier. The scatter of  $P_{NLM}$  and  $S_{NVC}$  in Layer 2 is much larger compared to Layers 1 and 3.

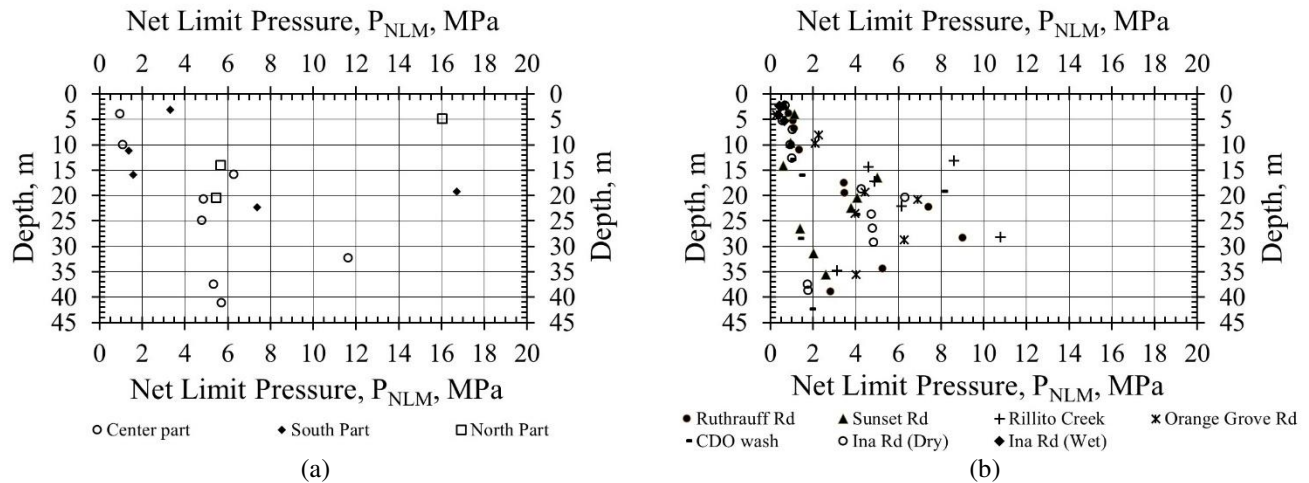


Figure 8.  $P_{NLM}$  Pressure profiles at (a) I10-I19 TI locations, (b) I10-ItoR locations.

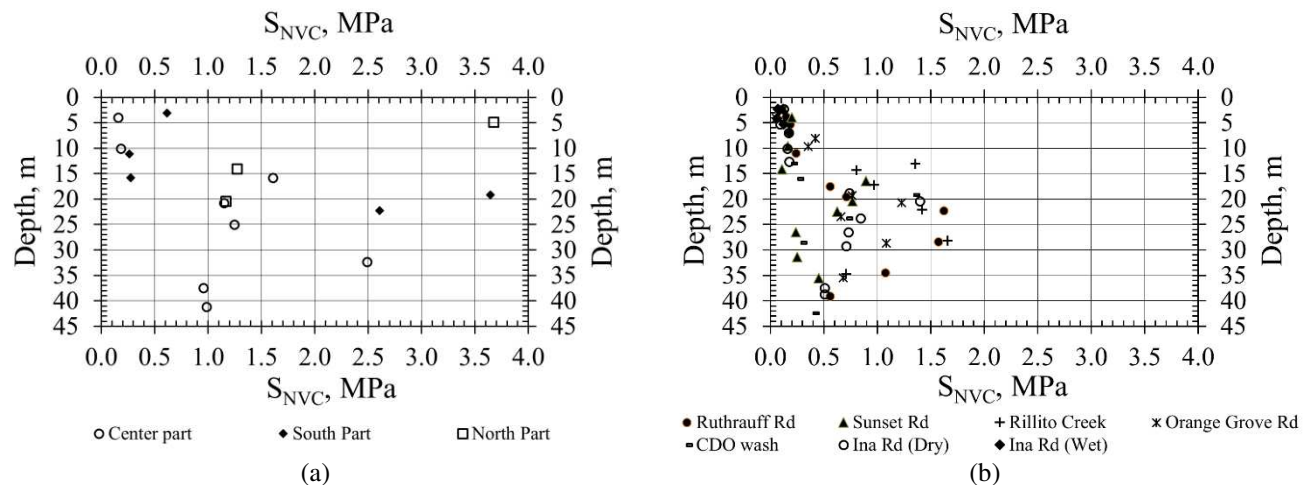


Figure 9.  $S_{NVC}$  profiles at (a) I10-I19 TI locations, (b) I10-ItoR locations.



If the foundation design were to be based solely on N-values then, as noted earlier, Layer 3 would give the impression of being the strongest from a geotechnical strength perspective because of the domination of refusal N-values in this layer. However, the  $P_f$ ,  $P_{NLM}$ , and  $S_{NVC}$  profiles indicate that Layer 3 is weaker than Layer 2, a trend that is corroborated by the  $K_o$  and LOCR profiles. The most significant aspect of the  $P_f$ ,  $P_{NLM}$ , and  $S_{NVC}$  profiles is that they provide tangible values for foundation design that cannot be gleaned from the refusal N-values which were frequently encountered, particularly in Layers 2 and 3. It would appear that the soil matrix within which larger particles such as gravels and cobbles are embedded controls the strength of soils in Layer 3. This underscores the fallacy of relying on refusal N-values for design, particularly for the types of alluvial soil deposits discussed in this paper.

## AXIAL GEOTECHNICAL RESISTANCE FOR DRILLED SHAFTS

The nominal unit side resistance,  $q_{SN}$ , and nominal unit base resistance,  $q_{BN}$ , for drilled shafts were evaluated using the two approaches identified herein as the “Pressuremeter” and “AASHTO-FHWA” approaches. Before presenting a comparison between these two approaches a brief discussion of each is provided below.

### The Pressuremeter Approach

The value of  $q_{SN}$  is obtained from a set of curves in a  $P_{LM}$  versus  $q_{SN}$  chart that was originally included in a French publication (LCPC-SETRA, 1985) and adapted by Briaud (1989) for Federal Highway Administration (FHWA). Similar charts are also included in Briaud (1992) and Clarke and Gambin (1998). More recent and updated guidance is provided in Briaud (2013). However, because the project design work was completed prior to availability of the updated guidance in Briaud (2013), this paper presents the results as they were evaluated and utilized during the projects using the chart in Clarke and Gambin (1998). A table, referenced as the chart-table herein, accompanies the chart to guide the choice of an appropriate curve. Each curve in the chart is applicable to a specific geomaterial, e.g., soft clay, dense sand, stiff marl, etc., and the type of deep foundation. Drilled shafts are referenced as drilled piles or bored concrete in Briaud (1989, 1992) and Clarke and Gambin (1998), respectively. To use this chart, first the USCS soil designations in Tables 3 through 13 were evaluated to select an appropriate geomaterial type from the options provided in the chart-table. Then, the  $P_{LM}$  value was used to select the appropriate curve to determine the value of  $q_{SN}$  for drilled shafts. The curves for “marl” were used for cases where the reaction to HCl is noted as “S” (i.e., strong) in the Notes column of Tables 3 through 13 which implies the  $CaCO_3$  content is significant. The final selection of the  $q_{SN}$  value was tempered using the author’s judgement based on experience with many projects in Tucson region and an evaluation of measured values of side resistance from over a hundred pullout tests for drilled soil nails, an axial load test at I10-I19 TI (Samtani and Liu, 2005), and several load tests at other locations in similar alluvial soil deposits.

The value of  $q_{BN}$  was obtained using  $q_{BN}=k(P_{NLM})+\sigma'_v$  (Briaud, 1989, 1992; Clarke and Gambin, 1998) where values for  $P_{NLM}$  ( $=P_{LM}-P_o$ ) and  $\sigma'_v$  for each test are given in Tables 3 to 13 and  $k=1.1$  is used for coarse-grained soils such as sand and gravel and  $k=1.2$  is used for fine-grained soils such as silt and clay.

The  $q_{SN}$  and  $q_{BN}$  values assume that the shaft is well constructed with intimate and firm contact of sound concrete ( $q_u>21$  MPa) with the undisturbed geomaterial on the side and base, i.e., without trapped loose material.

### The AASHTO-FHWA Approach

AASHTO, as used herein, refers to the Bridge Design Specifications of the American Association of State Highway and Transportation Officials (AASHTO) based on the Load and Resistance Factor Design (LRFD) methodology. Specifically, the guidance related to analysis of drilled shafts in Section 10 of AASHTO (2012) and AASHTO (2017) are referenced herein. The FHWA publications related to drilled shafts by O’Neill and Reese (1999) and Brown et al. (2010) are also referenced herein. The guidance for analysis of drilled shafts in AASHTO (2012) is based on O’Neill and Reese (1999) and is identified herein as the 2012 AASHTO-FHWA approach. The guidance for analysis of drilled shafts in AASHTO (2017) is based on Brown et al. (2010) and is identified herein as the 2017 AASHTO-FHWA approach.



In the 2012 AASHTO-FHWA approach, the analytical methods to estimate  $q_{SN}$  and  $q_{BN}$  are based on use of a depth-dependent side load-transfer coefficient,  $\beta$ , and  $N_{60}$  values. The  $N_{60}$  value is the hammer efficiency corrected N-value given as  $N_{60}=1.33N$ . To estimate  $q_{SN}$  and  $q_{BN}$  on projects that involve drilled shafts, ADOT's criteria for project development mandated the use of 2012 AASHTO-FHWA approach as modified by ADOT (2010). The value of  $q_{SN}$  is expressed as  $q_{SN}=\beta\sigma'_v$  where  $\beta$  is a load transfer coefficient expressed as  $\beta=X(1.5-0.245z^{0.5})$  for sands and drained soils,  $z$  is the depth in meters,  $X=1$  for  $N_{60}\geq 15$ ,  $X=N_{60}/15$  for  $N_{60}<15$ , and  $0.25<\beta<1.2$ . For gravelly sands or gravels with  $N_{60}\geq 15$ ,  $\beta=2.0-0.15z^{0.75}$  and  $0.25<\beta<1.8$ . In both cases, the limiting  $q_{SN}$  value is 0.2 MPa. The value of  $q_{BN}$  is expressed as  $q_{BN}=58N_{60}$  for  $N_{60}\leq 50$  and the limiting  $q_{BN}$  value is 2.9 MPa. In the 2012 AASHTO-FHWA approach, a soil deposit with  $N_{60}>50$  should be considered as an intermediate geomaterial (IGM). However, the analytical model for IGM in 2012 AASHTO-FHWA approach is based on residual soils of the Piedmont province in southeast US that was found not to be applicable for alluvial deposits in Arizona (ADOT, 2010). Therefore, for the soil conditions in Arizona, ADOT (2010) recommends that drained soils with  $N_{60}>50$  not be considered intermediate geomaterials (IGMs) but that the 2012 AASHTO-FHWA equations noted above be used assuming  $N_{60}=50$ .

In the 2017 AASHTO-FHWA approach, the evaluation of  $q_{BN}$  is based on the same equations as in the 2012 AASHTO-FHWA approach and therefore the same considerations for  $q_{BN}$  as noted above apply. However, for estimation of  $q_{SN}$ , the depth-dependent  $\beta$ -coefficient is replaced with a  $\beta$ -coefficient that is based on the approach proposed by Chen and Kulhawy (2002) and updated by Kulhawy and Chen (2007). In this approach the  $\beta$ -coefficient is a function of the effective friction angle,  $\phi'_f$  and OCR. The value of  $\phi'_f$  is determined using a correlation with  $N_{1-60}$  values where  $N_{1-60}$  value is the overburden corrected  $N_{60}$  value and the value of the preconsolidation stress to determine the OCR is based on  $N_{60}$  value. While 2017 AASHTO-FHWA documents note this as a "rational" approach, there are concerns with respect to its applicability to soil conditions such as those noted in this paper. The primary concern is the correlation between  $\phi'_f$  with  $N_{1-60}$  based on Kulhawy and Chen (2007) has a regression coefficient ( $r^2$  value) of 0.356 which as noted by Rollins et al. (2007) is a rather tenuous correlation leading to significant uncertainty in the  $\phi'_f$  value. Furthermore, this correlation is based on N-values obtained from case histories where large penetration tests (LPTs) and/or cross-correlations were made that justify usage of N-values in coarse soils. Most designers use SPTs with the 34.9 mm I.D., 50.8 mm O.D., and 457.2 mm long split spoon sampler that does not meet the definition of LPTs. Thus, for investigations based on SPTs, use of the 2017 AASHTO-FHWA approach necessitates use of additional correlations between LPTs and SPTs that have their own inherent uncertainties. With respect to refusal N-values obtained from standard SPTs it is unclear which value should be chosen for  $N_{1-60}$ . The choice of N-values to reflect refusal condition varies from 50 to 100 depending on the designer and this leads to significantly different values of  $q_{SN}$ , a situation that is compounded by the significant uncertainty in values of  $\phi'_f$  based on the correlation between  $\phi'_f$  with  $N_{1-60}$  that has poor underlying statistics to begin with. Earlier discussions about refusal N-values also emphasize the fallacy of relying on such values. The cumulative effect of these concerns is unreliable  $q_{SN}$  values from the 2017 AASHTO-FHWA approach for the types of soils discussed in this paper.

### Comparison of Pressuremeter and AASHTO-FHWA Approaches

Because of the various concerns related to the use of the 2017 AASHTO-FHWA approach for the type of soils encountered at the I10-I19 TI and I10-ItoR locations, this paper concentrates on comparison of the  $q_{SN}$  and  $q_{BN}$  values based on the pressuremeter approach with the 2012 AASHTO-FHWA approach that, as noted earlier, was mandated for project development by ADOT.

Figure 10 and Figure 11 show the variation of  $q_{SN}$  and  $q_{BN}$  for I10-I19 TI location and I10-ItoR location, respectively. In each figure, the data developed based on the pressuremeter approach are shown with open circles while the data developed based on the 2012 AASHTO-FHWA approach are shown as solid squares (for drained soils) and solid triangles (for gravelly soils and gravels) with the limiting 2012 AASHTO-FHWA maximum values being shown by a vertical dashed line. In Figure 10, additional data points based on the O-cell axial load test performed at I10-I19TI are displayed as solid circles. Details of the load test are provided in Samtani and Liu (2005). In Figure 10a, the load test data points are shown below a depth of 22 m because as noted in Samtani and Liu (2005), the strain gages above this depth indicated that the side resistance was not fully mobilized as the base failure occurred during the load test. The nominal base resistance corresponding to the failure condition in the axial load test is shown as the single data point with solid circle in Figure 10b at a depth of about 41 m.

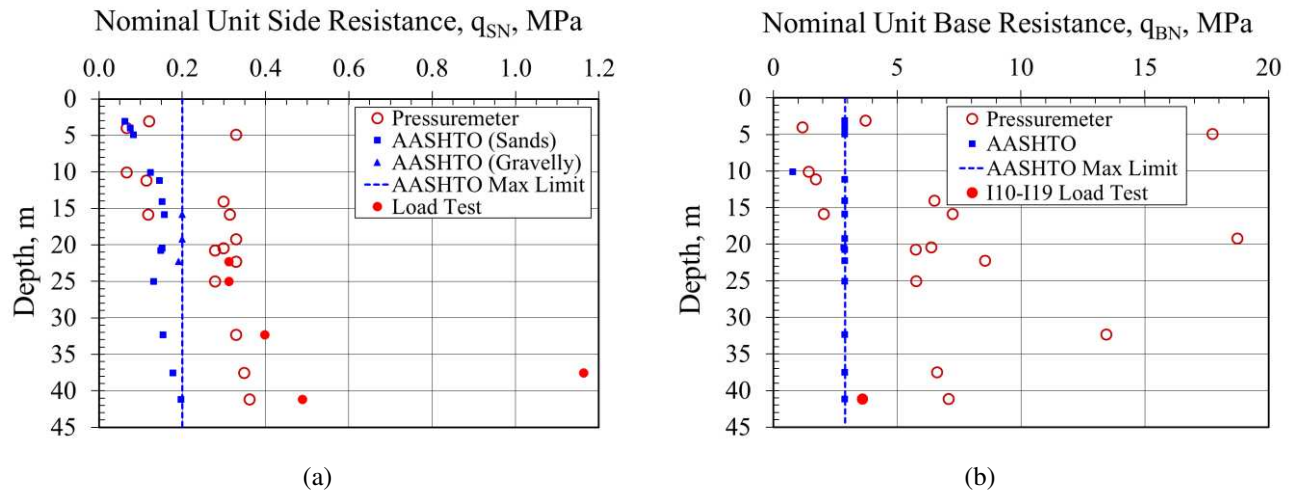


Figure 10. Profiles of Nominal Unit Resistance with Depth at I10-I19 TI location for (a) Side, (b) Base.

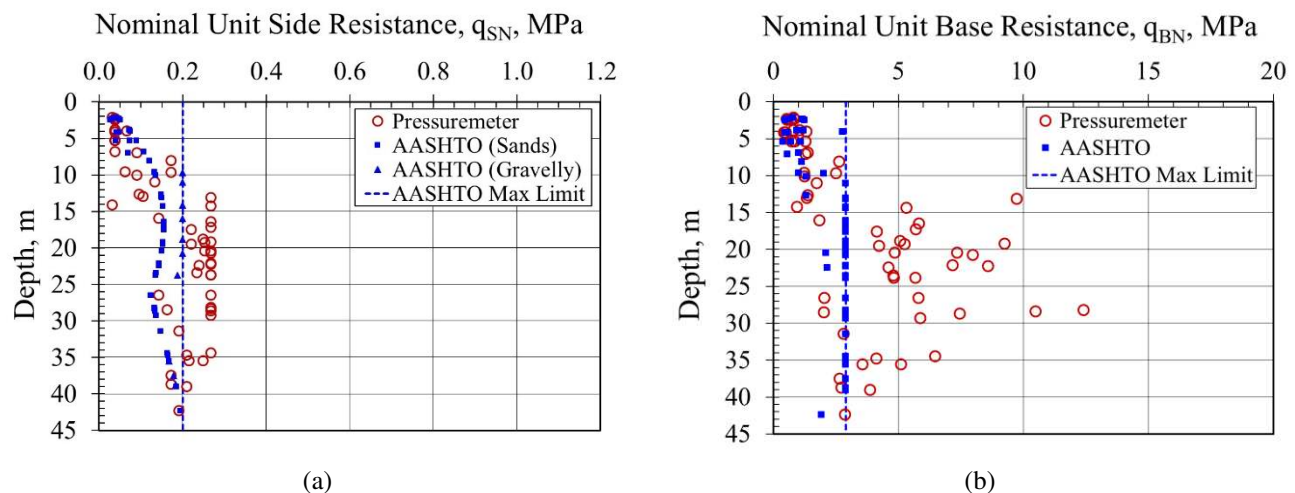


Figure 11. Profiles of Nominal Unit Resistance with Depth at I10-ItoR location for (a) Side, (b) Base.

The following observations are made based on the data shown in Figures 10 and 11:

- At the I10-I19 TI location, the data for  $q_{SN}$  from the load test correlates well with the estimated  $q_{SN}$  values from the pressuremeter approach. This is not surprising because the in situ state of stress and stress history are inherently reflected in the results of a pressuremeter and the load test. However, the estimate for base resistance,  $q_{BN}$ , from pressuremeter test is larger than that measured from the load test.
- The 2012 AASHTO-FHWA approach does not account for cementation or induration. In all the figures, the larger values based on pressuremeter tests may be indicative of the effect of cementation and/or induration on side resistance and base resistance.
- In the 2012 AASHTO-FHWA approach,  $q_{SN}$  is a direct function of depth with arbitrary limiting values which result in a linear  $q_{SN}$  profile below a depth of about 25 m with a bounding value of 0.2 MPa. These values were based on soils that are not cemented and/or indurated. The data points based on pressuremeter tests do not indicate a definite pattern with depth. This observation also may be indicative of the effect of cementation and/or induration on side resistance.



## “DRY AND WET” PRESSUREMETER TEST RESULTS

Figure 12 provides results of the dry and wet pressuremeter tests discussed earlier. The results are presented in terms of the radial pressure-radial strain format. The radial pressure is a representation of the radial soil resistance to radial deformation (expansion during loading and contraction during unloading). At depths of 2.3 m (Figure 12a) and 3.8 m (Figure 12b), the “wet tests” show a distinctly softer response compared to the “dry tests” in the sense that the radial pressure (radial soil resistance) at a given radial strain is smaller for the “wet” condition compared to the “dry” condition. In contrast, at the depth of 5.3 m (Figure 12c) similar stress-strain responses are observed for the “dry test” and the “wet test.”

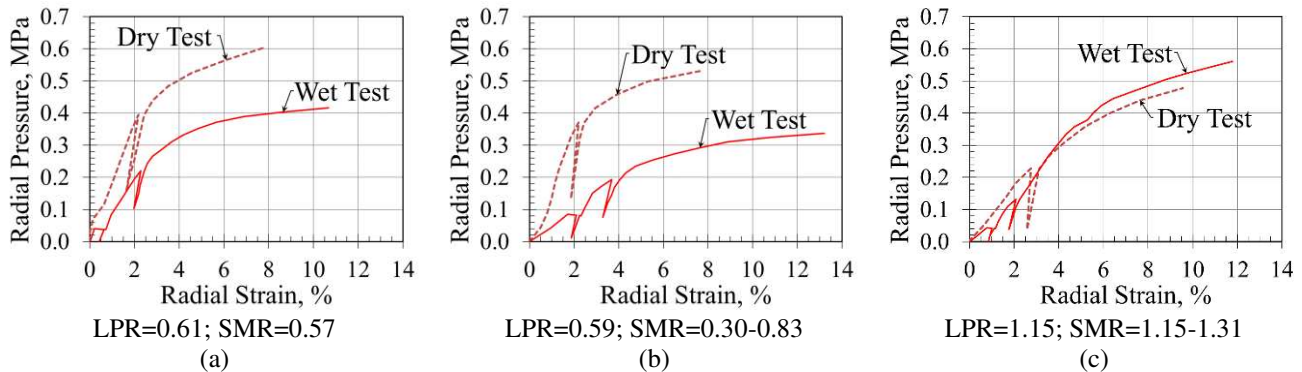


Figure 12. Dry and Wet Test Results at I10-Ina Road TI (a) Depth=2.3 m, (b) Depth=3.8 m, and (c) Depth=5.3 m.

In conjunction with the trends of the curves in Figure 12, the results of dry and wet pressuremeter tests can be interpreted using the following measures suggested by Smith and Rollins (1997).

- Limit Pressure Ratio, LPR, defined as  $P_{LMW}/P_{LMD}$ , where  $P_{LM}$  is the limit pressure as defined in Figure 3 and the subscripts “W” and “D” represent the “wet” and “dry” tests, respectively. The values of  $P_{LM}$  for wet tests are shown in top three rows of Table 11 and the corresponding values of  $P_{LM}$  for dry tests are shown in the three rows in Table 12. The LPR values are noted in Figure 12 for each set of dry and wet tests. A value of  $LPR < 1$  indicates that the nominal resistance of soil for the wet condition will be smaller than that for the dry condition. Thus,  $LPR=0.50$  indicates that a reduction in nominal strength of 50% can be expected if the soil under a given applied pressure is wetted.
- Soil Modulus Ratio, SMR, defined as  $E_{MW}/E_{MD}$ , where  $E_M$  is the initial (Menard) elastic soil modulus as defined in Figure 3 and the subscripts “W” and “D” represent “wet” and “dry” tests, respectively. The values of  $E_M$  for wet tests are shown in top three rows of Table 11 and the corresponding values of  $E_M$  for dry tests are shown in the three rows in Table 12. The SMR values are noted in Figure 12 with a range of values shown for Figures 12b and 12c because two values of  $E_M$  are noted in Table 11. A value of  $SMR < 1$  indicates that the soil is collapse-susceptible and the smaller the value of the SMR ratio the larger the severity of collapse. The SMR is also an indication of the increase in the strain (deformation) during collapse under a given applied pressure. Thus,  $SMR=0.50$  indicates the strain that could be experienced if the soil under a given applied pressure is wetted would be twice that for the case of no wetting.

In terms of LRFD, the LPR concept is more applicable to strength limit state evaluations, while the SMR concept is more applicable to the service limit state evaluation. However, the implications of increased settlement upon wetting of the soil can also have detrimental effects on the strength limit states of some elements, e.g., bearings and connections. Based on the values of LPR and SMR and the shapes of the curves in Figure 12, the results of the dry and wet tests indicate that the soils at depths of 2.3 m and 3.8 m exhibit “possible severe collapse” while the soils at a depth of 5.3 m are “not collapsible.” Thus, in general, the soils within about the upper 4 m at the I10-Ina TI location should be considered to have the potential to exhibit “possible severe collapse.”

The severity of collapse potential of the soil in the upper 4 m at the I10-Ina TI location was corroborated by laboratory tests performed on relatively undisturbed ring samples. The thick-walled ring sampler with dimensions as noted earlier was driven using the same automatic hammer used for SPTs. The ring samples were tested in accordance with ASTM D 5333 to measure



the collapse potential of soils. This test is used to evaluate the magnitude of one-dimensional (1-D) collapse that occurs when unsaturated soils are inundated with water. The results of ASTM D 5333 test are expressed in terms of a collapse index,  $I_c$ , that is defined as the difference in vertical strains before and after collapse under a constant applied stress of 200 kPa. ASTM D 5333 describes the degree of specimen collapse as “slight,” “moderate,” “moderately severe,” and “severe” for  $I_c$  values of 0.1 to 2%, 2.1 to 6%, 6.1 to 10%, and >10%, respectively. At the I10-Ina Road TI, 46 1-D collapse tests were performed and  $I_c$  values in the upper 4 m were found to range up to 11.5% indicating “severe” degree of collapse in accordance with the criteria in ASTM D 5333. Thus, excellent agreement between the laboratory and pressuremeter tests was observed. Overall, 19 and 103 1-D collapse tests were performed for I10-I19 TI and I10-ItoR locations, respectively, and it was determined that collapse-susceptible soils comprise a large portion of Layer 1. The evaluation of collapse potential from pressuremeter test has several advantages chief among which are (a) the pressuremeter test is axisymmetric (three-dimensional in radial direction) that is better suited for evaluation of axisymmetric drilled shafts in contrast to the laboratory 1-D tests where lateral strain is prevented, and (b) 1-D collapse tests on ring samples that are obtained by driving may not reflect the full collapse potential due to the soil structure being disturbed during the sample collection process in contrast to pressuremeter tests in carefully prepared test pockets that minimize the disturbance and thereby permits more realistic information on the collapse potential. Thus, the estimation of collapse potential from dry and wet pressuremeter tests is more representative of the in situ conditions.

## SUMMARY

A large database of pressuremeter tests along portions of Interstate 10 (I10) through Tucson, Arizona, has been presented in this paper. These tests were conducted in alluvial soil deposits that ranged from collapse-susceptible, variably cemented to indurated. In such formations, estimation of soil properties based on penetration resistance indicators such as N-values from Standard Penetration Tests (SPTs) is difficult. Varying content of gravels and cobbles provides additional complexity. In such conditions, sample recovery from SPTs is limited and refusal N-values occur. The fallacy of site characterization based on refusal N-values is observed. The case study demonstrated that pressuremeter tests are useful in assessing site stratigraphy as well as evaluating the effect of cementation, and/or induration. Estimated side and base resistances for drilled shafts based on the pressuremeter approach are presented and compared with the results of a large-scale axial load test and the 2012 AASHTO-FHWA approach. Evaluation of the collapse potential of soils using pressuremeter tests is also discussed and the results compared with the collapse potential based on 1-D laboratory tests.

Soils such as those discussed in this paper are found throughout the US desert southwest (e.g., Phoenix, Las Vegas, etc.) and elsewhere in the world. The estimated side and base resistance values reported in this paper when taken in conjunction with the in situ stress and stress history, cementation, and type of soil (i.e., data in Tables 3 through 13) can serve as a valuable resource for researchers and practitioners to judge and select appropriate design values for projects in soils in other geographical areas with similar history of soil deposition. Additional analyses to evaluate lateral response (so called p-y curves) and LRFD service limit state by developing resistance mobilization curves can be performed using the data in this paper; these additional evaluations were performed but due to space limitations are not presented in this paper.

## ACKNOWLEDGEMENTS

All the pressuremeter tests were performed under the direction and supervision of the author as part of ADOT projects while at URS Corporation (URS) during the I10-I19 TI project and at NCS Consultants, LLC (NCS) during the I10-ItoR project. Permission by ADOT to use the test results for this paper is acknowledged. The efforts of the late Professor Edward A. Nowatzki, Ph.D., P.E., D.GE, F.ASCE, who participated in the development of the I10-ItoR pressuremeter test program and provided significant guidance and technical reviews as Principal Engineer with NCS are noteworthy. The support of Joseph Harris, P.E. (NCS), and Kenton Watts (NCS) in collecting and cataloging subsurface data is acknowledged. The diligent pressuremeter testing and data processing efforts of Dale Baures, P.E., with URS (Denver, CO) are appreciated. Finally, the reviews provided by James C. Scott, P.E., Principal Engineer, AECOM (Denver, CO) during the development I10-I19 TI and I10-ItoR projects as well as the development of this paper are appreciated.

## REFERENCES

- American Association of State Highway and Transportation Officials (AASHTO) (2012). *AASHTO LRFD Bridge Design Specifications, 6<sup>th</sup> Edition*, Washington, D.C.
- American Association of State Highway and Transportation Officials (AASHTO) (2017). *AASHTO LRFD Bridge Design Specifications, 8<sup>th</sup> Edition*, Washington, D.C.



- 
- Arizona Department of Transportation (ADOT) (2010). *Interim Guidance – Design of Drilled Shafts in Gravels and Gravelly Soils Exhibiting Drained Behavior*, ADOT Policy Memorandum: ADOT DS-2,.
- Anderson, S. R. (1987). *Cenozoic Stratigraphy and Geologic History of the Tucson Basin, Pima County, Arizona*, United States Geological Survey, Water-Resources Investigations Report 87-4190, prepared in cooperation with the City of Tucson.
- American Society for Testing and Materials (ASTM) (2014). *Annual Book of ASTM Standards, Section 4, Volume 4.08, Soil and Rock (I): D420-D5876 and Volume 4.09, Soil and Rock (II): D5876-Latest*, West Conshohocken, PA.
- Baguelin, F., Jezequel, J. F., and Shields, D. H. (1978). *The Pressuremeter and Foundation Engineering*, Trans Tech Publications, Rockport, MA.
- Briaud, J-L. (1989). *The Pressuremeter Test for Highway Applications*, Federal Highway Administration, U.S. Department of Transportation, Washington, DC.
- Briaud, J-L. (1992). *The Pressuremeter*, A.A. Balkema, Brookfield, VT.
- Briaud, J-L. (2013). *Geotechnical Engineering: Unsaturated and Saturated Soils*, John Wiley & Sons, Inc., Hoboken, NJ.
- Brown, D. A., J. P. Turner, and R. J. Castelli. (2010). *Drilled Shafts: Construction Procedures and LRFD Design Methods—Geotechnical Engineering Circular No. 10*, National Highway Institute, Federal Highway Administration, U.S. Department of Transportation, Washington, DC.
- Brumund, W.F., Jonas, E., and Ladd, C.C. (1976). *Estimation of Consolidation Settlement – Manual of Practice*, Special Report 163, Transportation Research Board.
- Chen, Y-J. and F. H. Kulhawy. 2002. *Evaluation of Drained Axial Capacity for Drilled Shafts*, Geotechnical Special Publication No. 116, Deep Foundations 2002, ASCE, Reston, VA, 1200–1214.
- Clarke, B. G. (1995). *Pressuremeters in Geotechnical Design*, Blackie Academic & Professional.
- Clarke, B. G. and Gambin (1998). “Pressuremeter Testing in Onshore Ground Investigations: A Report by the ISSMGE Committee TC 16”, *Proc., 1<sup>st</sup> Int. Conf. on Site Investigations*, Atlanta, GA, USA, 2, 1429-1468.
- Davidson, E. S. (1973). *Geohydrology and Water Resources of the Tucson Basin, Arizona*, United States Geological Survey, Water-Supply Paper 1939-E, United States Geological Survey, prepared in cooperation with the City of Tucson, the U.S. Bureau of Reclamation, and the University of Arizona.
- Davidson, R. R. (1979). *Interpretation of the Pressuremeter Test*, Woodward-Clyde Consultants, Technical Memorandum No. 104-78.
- Gambin, M.P. and Jézequel, J.F. (1998). “A New Approach to the Menard PMT Parameters.” *Proc., 1<sup>st</sup> Int. Conf. on Site Investigations*, Atlanta, GA, USA, 2, 777-782.
- Gibson, R.E. and Anderson, W.F. (1961). “In-Situ Measurement of Soil Properties with the Pressuremeter.” *Civil Engineering and Public Works Review*, London, UK, 56, 615-618.
- Jaky, J. (1944). “The coefficient of earth pressure at rest.” *Journal of the Society of Hungarian Architects and Engineers*, 7, 355-358.
- Kulhawy, F.H. and Y-R Chen. 2007. “Discussion of ‘Drilled Shaft Side Resistance in Gravelly Soils’ by Kyle M. Rollins, Robert J. Clayton, Rodney C. Mikesell, and Bradford C. Blaise,” *Journal of Geotechnical and Geoenvironmental Engineering*, ASCE, 133(10), 1325–1328.
- Nowatzki, E. A., and Almasmoum, A. A. (1988). “A Method for Estimating the Excavatability of Caliche.” *Geotechnical Testing Journal*, American Society of Testing and Materials, GTJODJ, 11(2), 148-154.
- Laboratoire Central des Ponts et Chaussées, Service d’Etudes Techniques des Routes et Autoroutes (LCPC-SETRA) (1985). *Regles de Justification des Fondations sur Pieux a Partir des Resultats des Essais Pressiométriques*.
- O’Neill, M. W. and L. C. Reese. 1999. “Drilled Shafts: Construction Procedures and Design Methods”, *Publication No. FHWA-IF-99-025*, Federal Highway Administration, U.S. Department of Transportation, Washington, DC.
- PAG (2019). “Arizona MapGuide Map”, *Pima Association of Governments*, Tucson, AZ <<http://webcms.pima.gov/cms/one.aspx?portalId=169&pageId=34155>> (May 26, 2019).
- Parker, J.T.C (1995). “Channel change on the Santa Cruz River, Pima County, Arizona, 1936-1986” *United State Geological Survey Water-Supply Paper 2429*.
- Rollins, K.M., Clayton, R.J., Mikesell, R.C., and Blaise, B.C. (2007). “Closure to ‘Drilled Shaft Side Resistance in Gravelly Soils’ by Kyle M. Rollins, Robert J. Clayton, Rodney C. Mikesell, and Bradford C. Blaise,” *Journal of Geotechnical and Geoenvironmental Engineering*, ASCE, 133(10), 1328–1331.
- Samtani, N. C. and Liu, J. J. (2005). “Use of In-situ Tests to Design Drilled Shafts in Dense and Cemented Soils.” *GEOFRONTIERS 2005, Geotechnical Special Publications 132 – Advances in Deep Foundations (CD-ROM)*, an ASCE Geotechnical Specialty Conference: Austin, TX.
- Smith, T. D. and Rollins, K. M, (1997). “Pressuremeter Testing in Arid Collapsible Soils.” *Geotechnical Testing Journal*, American Society of Testing and Materials, GTJODJ, 20(1), 12-16.
-



INTERNATIONAL JOURNAL OF  
**GEOENGINEERING  
CASE HISTORIES**

*The Journal's Open Access Mission is  
generously supported by the following Organizations:*



Access the content of the *ISSMGE International Journal of Geoengineering Case Histories* at:  
[www.geocasehistoriesjournal.org](http://www.geocasehistoriesjournal.org)